ELSEVIER

Journal of Hazardous Materials 140 (2007) 205–210

Journal of Hazardous Materials

www.elsevier.com/locate/jhazmat

Oxidation treatment of diesel soot particulate on $Ce_xZr_{1-x}O_2$

Ling Zhu [a,*], Junjie Yu [b], Xuezhong Wang [c]

[a] *Department of Environmental Engineering, Beijing Institute of Petrochemical Technology, Qingyuan North Road 19, Beijing, 102617, PR China*
[b] *Research Center of Eco-Environmental Sciences, Chinese Academic Sciences, Shuangqing Road 18, Beijing 100085, PR China*
[c] *Chinese Research Academy of Environmental Sciences, Dayangfang Road 8, Beijing 100012, PR China*

Received 9 December 2005; received in revised form 28 May 2006; accepted 19 June 2006
Available online 21 June 2006

Abstract

Catalytic oxidation of diesel soot particulate on $Ce_xZr_{1-x}O_2$ catalysts was investigated. Results indicated that Ce/Zr ratios had a significant influence on the catalytic activities. Compared with the ignition temperature (T_i) of uncatalyzed soot combustion, T_i of $Ce_{0.5}Zr_{0.5}O_2$ with the best catalytic behavior decreased by 80 °C. The reactant gas compositions (O_2, H_2O and NO) affected the catalytic activities too. O_2-TPD, TG–DTA and XPS characterization results showed that $Ce_xZr_{1-x}O_2$ released lattice oxygen continuously to promote the soot combustion even no gas oxygen occurred in the reaction atmosphere. The mechanisms of spill-over and reduction/oxidation functioned synergistically for soot catalytic combustion.

Keywords: $Ce_xZr_{1-x}O_2$ solid solution; Soot; Catalytic oxidation; Reaction mechanism

1. Introduction

The emissions of diesel engines are known to be hazardous pollutants for human health. One of the most dangerous components of diesel exhausts is particulate, which consists of agglomerates of small carbon particles with numbers of different hydrocarbons and sulphates adsorbed on their surfaces. A possible way to reduce particulate emission lies in filtering it with trap, and continuously burning out it on the presence of catalyst system which promotes particulate combustion at relatively low temperatures of the exhaust emission (below 400 °C).

During the past decades, several catalysts were reported in references for soot oxidation, including perovskite-related oxides and spinel oxides [1,2], chloride-containing mixtures [3,4], eutectic mixtures of oxides [5,6], and noble metal catalysts [7,8]. However, only a few works involved soot combustion over rare earth oxide and its combined catalysts, relatively rare systemic research work reported soot combustion over Ce/Zr oxide catalysts.

Due to its oxygen storage capability (OSC) and redox properties (Ce^{4+}/Ce^{3+}), CeO_2 had been widely used as oxygen storage material in three-way catalyst (TWC) [9]. Furthermore, as a main compound of the fuel additive, in this case cerium should be collected on the filter with the form of ceria, which promotes the combustion of soot trapped in the filter [10]. Relevant research shows that zirconium prevents the growth of CeO_2 crystallites at high temperatures and improves the thermal stability of CeO_2 [11].

This paper described the catalytic activities of Ce/Zr series catalysts ($Ce_xZr_{1-x}O_2$) for catalytic soot combustion in various feed gas compositions (O_2, NO, H_2O). Catalyst structures were characterized by XRD and XPS techniques; the mechanism of soot combustion on $Ce_{0.5}Zr_{0.5}O_2$ was explored by O_2-TPD and TG–DTA.

2. Experimental

2.1. Materials preparation

$Ce_xZr_{1-x}O_2$ catalysts with different Ce/Zr ratios ($x = 0$, 0.3, 0.5, 0.7, 1.0) were prepared by coprecipitation of aqueous $Ce(NO_3)_3$ and $ZrO(NO_3)_2$ solutions with NH_3H_2O as a coprecipitation agent. The precipitates were dried at 100 °C and calcined in the air at 700 °C for 4 h.

2.2. Materials characterizations

The oxygen storage capacity (OSC) was estimated by the thermo-gravimetric analysis (TAS-300, Rigaku Co., Ltd.) [12].

* Corresponding author. Tel.: +86 10 81292291; fax: +86 10 81292291.
E-mail addresses: zhuling75@bipt.edu.cn, zhuling7519@163.com (L. Zhu).

0304-3894/$ – see front matter © 2006 Elsevier B.V. All rights reserved.
doi:10.1016/j.jhazmat.2006.06.055

The textural properties of the samples were measured by nitrogen adsorption/desorption at liquid nitrogen temperature in a NOVA 1200 high-speed gas sorption analyzer.

XRD analysis was performed on a D/max 2400 diffractometer (Rigaku Co., Ltd.) with Cu Kα radiation. Diffraction peaks of crystalline phases were compared with those of standard compounds reported in the JCPDS Data File.

O_2 temperature programmed desorption (O_2-TPD) was carried out by a conventional TPO apparatus connected to a chromatography according to the following procedure: catalyst sample was heated to 500 °C in the helium atmosphere and held for 1 h, then cooled down to room temperature and started the TPD test for two circles. The temperature of reactor bed was raised with a heating rate of 10 °C/min and all the TPO experiments were conducted in the helium atmosphere.

X-ray photoelectron spectra (XPS) were acquired with a VGESCALAB MKII spectrometer equipped with a hemispherical electron analyzer and Mg Kα X-ray source. All binding energies (B.E.) were referenced to the C 1s line at 284.6 eV, which provided binding energy values with an accuracy of ±0.2 eV.

2.3. Activity evaluation

Model soot was the Printex-U supplied by Degussa. Before reaction, soot was carefully mixed with the catalyst, in the ratio of 1/10. Mixing in this way resulted in a "loose" contact between the catalyst and soot, which was assumed to be close to that found in practical cases.

The activities were evaluated in temperature programmed oxidation (TPO) reactor. Soot-catalyst mixture (110 mg) was placed into the quartz reactor ($\varphi = 10$ mm) and performed in the range 30–700 °C (at a heating rate of 10 °C/min) in the flowing gas (10%O_2/N_2, with a flow rate of 500 ml/min). A non-dispersive IR gas analyzer (TY-9800A) was used to monitor the concentration of CO_2 continuously.

About 1000 ppm NO and 7% H_2O were added into 10%O_2/N_2 to explore the effect of the reactant gas composition on the catalytic activity of $Ce_{0.5}Zr_{0.5}O_2$.

3. Results and discussion

3.1. OSC and BET surface area

Table 1 shows the OSC properties and BET surface area of the $Ce_xZr_{1-x}O_2$ samples. When ZrO_2 added into CeO_2, its OSC is obviously increased and the OSC of $Ce_{0.5}Zr_{0.5}O_2$ reaches the maximum. OSC is irrelevant to the surface area.

Table 1
Characteristic parameters of $Ce_xZr_{1-x}O_2$ catalysts

Catalyst sample	BET surface area (m^2/g)	OSC (μmol O_2/g)
CeO_2	58.22	137.09
$Ce_{0.7}Zr_{0.3}O_2$	130.82	396.05
$Ce_{0.5}Zr_{0.5}O_2$	132.61	439.85
$Ce_{0.3}Zr_{0.7}O_2$	121.8	277
ZrO_2	30.9	0

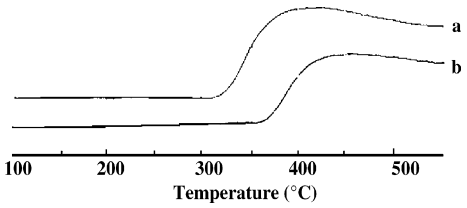

Fig. 1. O_2-TPD curves of $Ce_{0.5}Zr_{0.5}O_2$: (a) the first test; (b) the second test.

3.2. XRD analysis

XRD results (XRD patterns were not given in this paper) indicate that the structure of CeO_2 corresponded to a single phase of fluorite-type structure. When ZrO_2 added into CeO_2, the related peaks move to higher angle value and the peak become broader; the crystal phase of $Ce_{0.3}Zr_{0.7}O_2$ shift from cubic to tetragonal construction [13]. Whatever the percentage of ZrO_2 added, no ZrO_2 phases are detected, therefore, $Ce_xZr_{1-x}O_2$ samples are in a homogeneous phase.

3.3. O_2-TPD analysis

Generally, there are three kinds of active oxygen species: α, β, and γ on surface of Ce–Zr solid solution. α O species has a lower desorption temperature (<350 °C), which is assigned to the chemical adsorption oxygen; γ O species has a higher desorption temperature(>750 °C), being assigned to the oxygen in crystal lattice. However, desorption temperature of β O species is between these two desorption temperatures, which is related with oxygen defect and is considered as partial crystal oxygen [14].

The O_2-TPD curves of $Ce_{0.5}Zr_{0.5}O_2$ were shown in Fig. 1. The peak temperature matches up to the desorption temperature of β O species, so these peaks represented some kind of β O species. It could be seen from these curves that the catalyst released oxygen continuously when its temperature raised. This is an important character when the catalyst was used for soot combustion in the condition of lacking of oxygen as oxidant.

3.4. TPO experiment

The activity of catalyst in TPO evaluation was represented by the ignition temperature (T_i) and the peak temperature (T_p). T_i and T_p were defined as the temperatures where the concentration of CO_2 exceeds 20 ppm at 5 °C interval and where the maximum CO_2 emitted. According to the Redhead method, we estimated the activation energy of soot combustion by the following equations [15]:

$$A\frac{E_a}{RT_p}e^{-Ea/RT} = \frac{\alpha E_a}{RT_p^2}$$

where A is the Arrhenius pre-exponential, E_a the activation energy terms and α is the heating rate.

The TPO results were shown in Table 2 and Fig. 2. Without catalyst, the soot oxidation begins at 490 °C and the T_p

Table 2
Soot oxidation activities on various catalysts in TPO evaluation

Catalyst	T_i (°C)	T_p (°C)	ΔT (°C)	E_a (kJ/mol)
Without catalyst	490	595	105	159.43
CeO_2	445	573	128	155.20
$Ce_{0.7}Zr_{0.3}O_2$	425	543	118	149.47
$Ce_{0.5}Zr_{0.5}O_2$	410	525	110	146.04
$Ce_{0.3}Zr_{0.7}O_2$	460	559	119	152.53
ZrO_2	490	595	105	159.43

is around 595 °C; ZrO_2 shows no catalytic activity for soot combustion. The performances of Ce-based catalysts are obviously enhanced. Compared with the result of uncatalyzed soot combustion, T_i and T_p on Ce-based catalysts shift to lower temperature by 30–80 °C at the different Ce/Zr ratios. $Ce_{0.5}Zr_{0.5}O_2$ has the best catalytic performance, its T_i and T_p decrease by 80 and 70 °C, respectively. The calculated results of reaction energies are accordant with the catalytic activities.

The introduction of ZrO_2 (seven-fold coordination) into CeO_2 (eight-fold coordination) may lead to the reduction of element numbers in crystal grain and the aberrance of adjacent oxygen atom, which makes it easier to deviate from the crystal lattice to become the interstice atom [16]. At the same time, the effective ionic radii of Ce^{4+}, Ce^{3+} and Zr^{4+} are 0.097, 0.114 and 0.084 nm, respectively [16]. The introduction of the small size zirconium ions into the cerium framework may compensate for the volume expansion, hence facilitate the process of valence change. As a result, T_i of soot combustion decreases gradually. T_i of soot on $Ce_{0.5}Zr_{0.5}O_2$ is lowered by 80 °C. This may contribute to the number of adjacent oxygen coordination around Zr^{4+} decreasing from 7 to 6. On the contrary, introducing more ZrO_2 to CeO_2, $Ce_{0.3}Zr_{0.7}O_2$ becomes a new tetragonal structure: the increase of the lattice parameters *c*/*a* and the augment of crystal anisotropy [17], which blocks the oxygen release and move. Therefore, T_i and T_p of $Ce_{0.3}Zr_{0.7}O_2$ catalyst are increased.

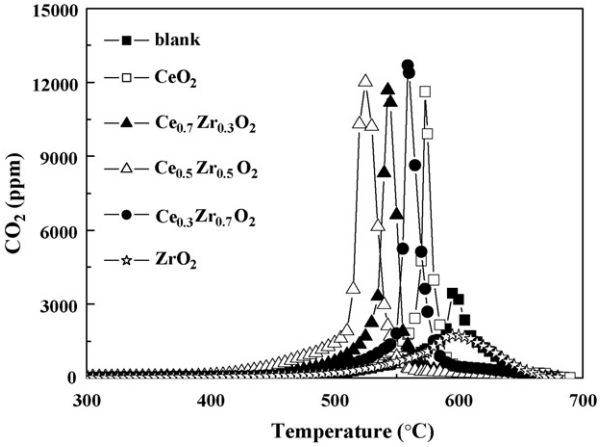

Fig. 2. Catalytic performance of $Ce_xZr_{1-x}O_2$ for soot oxidation in TPO.

Table 3
Effect of feed gas composition on the catalytic performance of $Ce_{0.5}Zr_{0.5}O_2$ for soot combustion

Feed gas composition	T_i (°C)	T_p (°C)	ΔT (°C)
$10\%O_2$–N_2	410	525	115
$10\%O_2$–$7\%H_2O$–N_2	410	525	115
$10\%O_2$–1000 ppm NO–N_2	380	500	120
$10\%O_2$–1000 ppm NO–$7\%H_2O$–N_2	385	500	115

3.5. Effect of feed gas compositions on the catalytic performance of $Ce_{0.5}Zr_{0.5}O_2$ for soot oxidation

3.5.1. Effect of feed gas compositions on the soot combustion without catalyst

As shown in Table 3 and Fig. 3, in the absence of NO, the addition of H_2O has little effect on the T_i and the reaction rate. This phenomenon is consistent with the reported results that the experimental activation energies of soot combustion without catalysts in $10\%O_2$–N_2 and $10\%O_2$–$10\%H_2O$–N_2 are 168 and 169 kJ/mol, respectively [18]. The reaction of NO oxidation is an exothermic process, and NO_2 concentration and rate of soot oxidation with NO_2 do not increase with the raising of temperature. So, the addition of NO does not affect the T_i of soot combustion. On the contrary, the competitive reaction with active oxygen between soot and NO results in the increase of T_p by 5–25 °C.

3.5.2. Effect of O_2 concentration on the catalytic performance of $Ce_{0.5}Zr_{0.5}O_2$ for soot oxidation

When the concentration of O_2 exceeds 8.5%, there was no influence on soot combustion and T_i and T_p remain at 410 and 525 °C (seen from Fig. 4). When the concentration of O_2 is 1–8.5%, with the decrease of O_2 concentration, T_i has not been changed; however, T_p increases from 525 to 580 °C and the reaction rate slows down. Inui et al. [19] reported that the concentration of O_2 greatly affected on the rate-determined step during the course of soot combustion. The absorption of oxygen on the catalysts surface has a very quick velocity and a

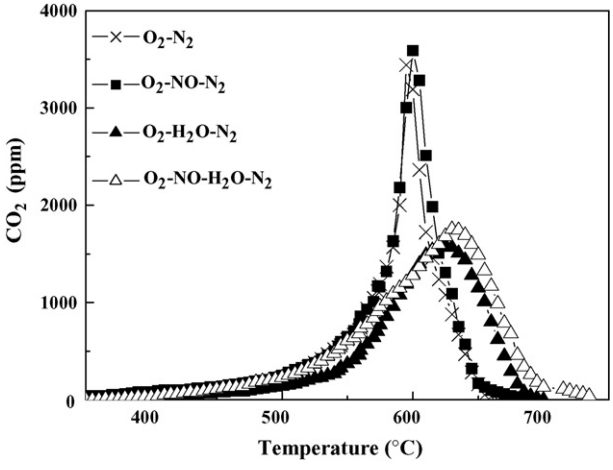

Fig. 3. Effect of the composition of reaction gas on the soot oxidation without catalysts.

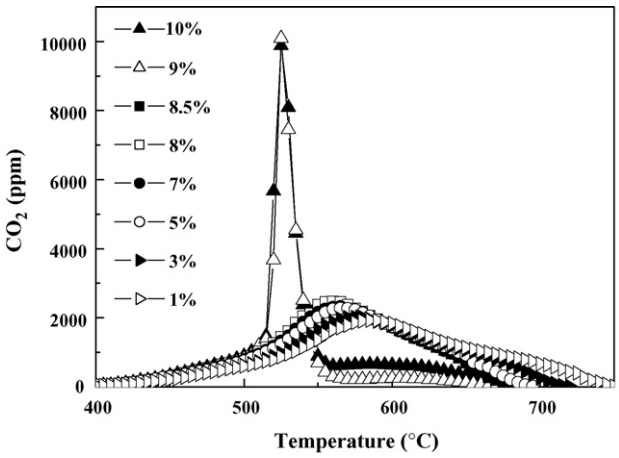

Fig. 4. Effect of O_2 concentration on catalytic soot oxidation on $Ce_{0.5}Zr_{0.5}O_2$.

very high intensity. When the reaction atmosphere has a high O_2 concentration (>8.5%), the rate-determined step is the oxygen transference on the catalyst surface, and compared with the active oxygen species released from catalysts, desorption gaseous oxygen is the main surface active oxygen species. When the reaction atmosphere contains the low concentration of O_2 (<8.5%), the rate-determined step is the absorption of O_2 on the catalysts surface and the transference velocity of O_2 inside the catalysts is very quick. With the decrease of O_2 concentration, the quantity of absorption oxygen reduces and the active oxygen species reduces accordingly. Therefore the oxidation velocity of CeO_{2-Y} becomes slow, which influences the rate of releasing oxygen. As shown in Fig. 5, with the fall of O_2 concentration, the rate of soot combustion gradually lowers and the T_p increases.

3.5.3. Effect of H_2O and NO

From Fig. 5 we found that the addition of 7%H_2O has no effect on soot combustion over $Ce_{0.5}Zr_{0.5}O_2$. It means that the Ce–Zr solid solution has an excellent water tolerance and thermal stability. When NO is added to the reactant gas, T_i decreases by 30 °C and the TPO curves becomes relatively flat. It indicates that NO plays an important role in soot combustion on $Ce_{0.5}Zr_{0.5}O_2$. The active oxygen (O^*) formed on the

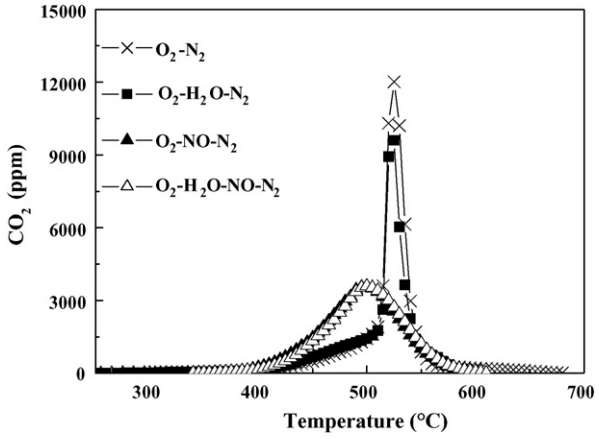

Fig. 5. Effect of the composition of reaction gas on the soot oxidation on $Ce_{0.5}Zr_{0.5}O_2$.

$Ce_{0.5}Zr_{0.5}O_2$ surface reacts with NO and converts into NO_2. NO_2 has spatial configuration and the N–O band in the NO_2 molecule is easy to be broken, therefore the oxidation activity of soot with NO_2 is higher than O_2. T_i decreases by 30 °C, which may be due to lower reaction temperature of soot and NO_2 (about at 275 °C in term of thermodynamics calculation). Along with soot combustion, both NO and CO_2 are absorbed in the alkaline sites and the absorption–desorption rate of intermediate compound decreases. Due to O^* competition between NO and soot, the combustion course becomes slower. Baker and Chludzinski [20] reported that the process of CO_2 formation from the interaction between NO_2 and proceeds through the oxidation of active sites on the soot surface, via abstraction of oxygen atoms from NO_2 to produce partially oxidized surface species (>C=O) and NO. Oi-Uchisawa et al. [8] also found the same phenomenon for soot combustion over Pt/SiO_2 in the present of NO.

3.6. Mechanistic aspect

The oxygen involved for soot combustion comes from two aspects as follow: the gaseous oxygen and the oxygen released from catalysts; thus the soot oxidation on $Ce_xZr_{1-x}O_2$ catalyst should be occurred the following two reaction process:

$$C + O_2 \rightarrow CO_2 \quad (1)$$

$$CeO_2 + C \rightarrow CO + CO_2 + CeO_{2-Y} \quad (2)$$

The better catalytic activity may contribute from the dissociation centres for the adsorption oxygen ($O_{2\,ads}$) provided by the metal oxides [21]. On the surface of CeO_2, $O_{2\,ads}$ (with surplus odd 2d electrons) bond with Ce (with empty orbits) and give bonded oxygen in the form of π bond, the outer electron cloud of oxygen atom become unsymmetrical. Accepted external energies, π bond would be broken and dissociated into various surface O species (O^*), especially bonded with the Ce atom near the $Ce_xZr_{1-x}O_2$ surface defect. To Eq. (1), gaseous oxygen is absorbed on the catalyst surface (Eq. (3)) and the absorption oxygen is dissociated to a series of surface oxygen species (O^*), such as O radicals ($O^\bullet$), superoxide radicals (O^-, O_2^-, O_2^{2-}, etc.) (Eq. (4)). These O^* are transferred to the soot surface through the spill-over effect, then attack the soot to give an oxygen-containing active intermediate (C–O^*s), $CO_{(ads)}$ and $CO_{2(ads)}$ (Eq. (5)). The detail of C–O^*s is still not clear at present, but the presence of such an oxygen-containing reactive surface complex is confirmed on the char surface after reaction with gaseous oxygen. Decomposition of the C–O^*s results in the formation of $CO_{(ads)}$ and $CO_{2(ads)}$ (Eq. (6)), the $CO_{(ads)}$ and $CO_{2(ads)}$ are desorbed from the soot surface into the air at last

$$O_2 \rightarrow O_{2(ads)} \quad (3)$$

$$O_{2(ads)} \rightarrow 2O \rightarrow 2O^* [O^\bullet, O^-, O_2^-, O_2^{2-}] \quad (4)$$

$$O^* + C \rightarrow C\text{–}O^*s + CO_{(ads)} + CO_{2(ads)} \quad (5)$$

$$C\text{–}O^*s + CO_{(ads)} + O^* \rightarrow CO_{2(ads)} \quad (6)$$

Meanwhile, $Ce_xZr_{1-x}O_2$ catalysts have a high oxygen storage capacity. Through spill-over effect, oxygen released from

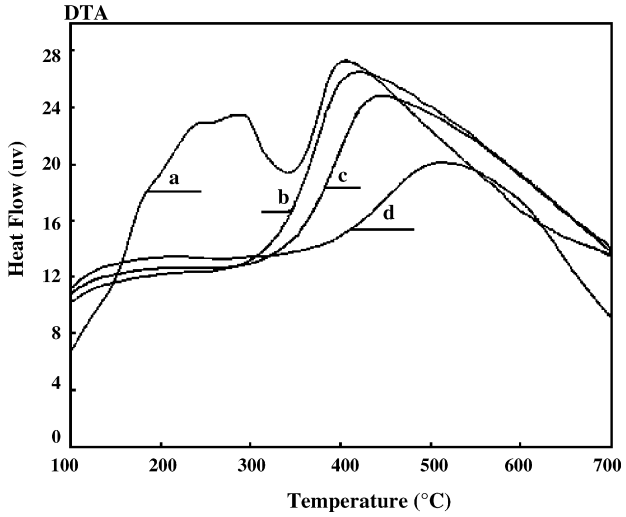

Fig. 6. TG–DTA result of soot combustion on $Ce_{0.5}Zr_{0.5}O_2$ in N_2 atmosphere: (a) the first test; (b) the second test; (c) the third test; (d) the fourth test.

$Ce_xZr_{1-x}O_2$ (Eq. (7)) react with soot and form CO and CO_2 (Eqs. (5) and (6)); at the same time, CeO_{2-Y} in reductive state are oxidized to CeO_2 (Eq. (8)). This process is preceded through reduction/oxidation mechanism:

$$CeO_2 \rightarrow CeO_{2-Y} + xO^* \quad (7)$$

$$O^* + C \rightarrow C\text{–}O^*s + CO_{(ads)} + CO_{2(ads)} \quad (5)$$

$$C\text{–}O^*s + CO_{(ads)} + O^* \rightarrow CO_{2(ads)} \quad (6)$$

$$CeO_{2-Y} + YO^* \rightarrow CeO_2 \quad (8)$$

The two mechanisms of spill-over and reduction/oxidation function synergistically for soot combustion [21].

To prove the existence of reduction/oxidation function, TG–DTA curves of $Ce_{0.5}Zr_{0.5}O_2$ of four test circles in high purity nitrogen atmosphere were conducted and the results were shown in Fig. 6.

There are two exothermic peaks on DTA curve in the first test cycle, however only one peak in the other cycles. The first peak (200–300 °C) in the first circle can be ascribed to the reaction of soot with absorbed oxygen. The second peak (above 300 °C) is consistent to the peak in the O_2-TPD experiment under the He atmosphere (Fig. 1). At the same time, the peak temperature moves to higher value as the test cycle increases. The second peak is due to the reaction between the soot and desorbed lattice oxygen (so-called "stored" oxygen). Along with the consumption of oxygen, the energy needed to release residual oxygen in lattice becomes higher, which is accordant with the increase of peak temperature and the decrease of peak area in the following reactions cycles.

$Ce_{0.5}Zr_{0.5}O_2$ and $Ce_{0.5}Zr_{0.5}O_2$ after the above TG experiments are also analyzed by XPS. The O 1s spectra are fitted with two peak contributions, referred to as O_I and O_{II} components, as showed in Table 4 and Fig. 7. The major peak component O_I with B.E. at 528.9–529.7 eV is characteristic of lattice oxygen. Component O_{II} with B.E. at 531.0–532.0 eV belongs most likely to the adsorbed oxygen or the surface hydroxyl species

Table 4
Quantitative aspects of analyses of sample by XPS

Catalyst	O_I[a] (%)	O_{II}[b] (%)	Ce^{4+}/Ce^{3+} (%)
$Ce_{0.5}Zr_{0.5}O_2$	71.15	28.85	62
$Ce_{0.5}Zr_{0.5}O_2$ (after TG experiment)	81.97	18.03	51

[a] The lattice oxygen.
[b] The adsorbed oxygen or the surface hydroxyl species.

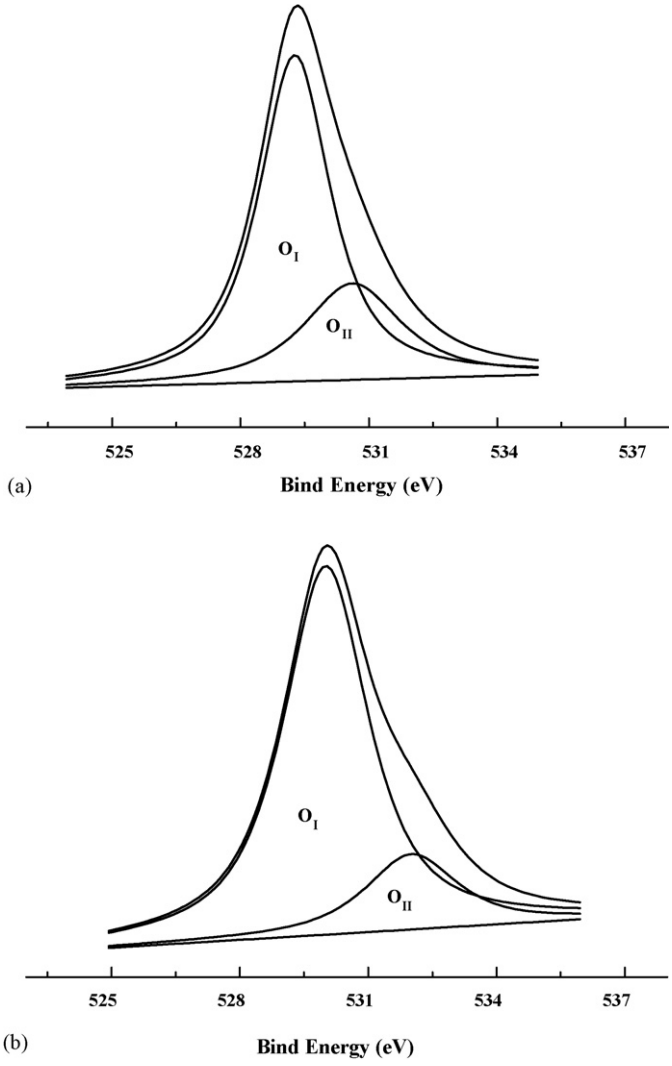

Fig. 7. XPS O 1s spectra of the samples: (a) fresh $Ce_{0.5}Zr_{0.5}O_2$; (b) $Ce_{0.5}Zr_{0.5}O_2$ after the above TG reaction.

[22]. Compared with the fresh sample, the O_{II}% in the sample after TG experiment is decreased from 28.85 to 18.03% and the Ce^{4+}% is changed from 62 to 51% accordingly. These results indicates that the O_I takes part in the reaction of soot combustion and part of O^* are offered by the deoxidizing CeO_2 to Ce_2O_3, which is consistent with the above TG experiment.

4. Conclusions

$Ce_xZr_{1-x}O_2$ catalysts promote the soot combustion and have good water tolerance and thermal stability. Ce/Zr ratios affect

the catalytic activities greatly and the T_i lowers by 80 °C on $Ce_{0.5}Zr_{0.5}O_2$ with the best catalytic performance. The concentration of O_2 has a significant effect on the rate-determined step during soot combustion. NO improves the catalytic activity of $Ce_{0.5}Zr_{0.5}O_2$ and the T_i decreases by 30 °C. The oxygen storage capacity of $Ce_{0.5}Zr_{0.5}O_2$ is the main season for soot combustion in an atmosphere lack of oxygen. β oxygen participates in the soot combustion reaction and the mechanisms of spill-over and reduction/oxidation function synergistically.

References

[1] Y. Teraoka, K. Kanada, S. Kagawa, Synthesis of La–K–Mn–O perovskite-type oxides and their catalytic property for simultaneous removal of NO_x and diesel soot particulates, Appl. Catal. B: Environ. 34 (2001) 73–78.

[2] W.F. Shangguan, Y. Teraoka, S. Kagawa, Simultaneous catalytic removal of NO_x and diesel soot particulates over ternary AB_2O_4 spinal-type oxide, Appl. Catal. B: Environ. 8 (1996) 217–227.

[3] J.A. Neeft, W. Schipper, G. Mul, M. Makkee, J.A. Moulijn, Feasibility study towards a Cu/K/Mo/Cl soot oxidation catalysts for application diesel exhaust gases, Appl. Catal. B: Environ. 11 (1997) 365–382.

[4] G. Mul, J.P.A. Neeft, F. Kapteijn, M. Makkee, J.A. Moulijn, Soot oxidation catalyzed by a Cu/K/Co/Cl catalyst: evaluation of the chemistry and performance of the catalyst, Appl. Catal. B: Environ. 6 (1995) 339–352.

[5] S.J. Jelle, B.A.A.L. van Setten, M. Makkee, J.A. Moulijn, Molten salts as promising catalysts for oxidation of diesel soot: importance of experimental conditions in testing procedures, Appl. Catal. B: Environ. 21 (1999) 35–49.

[6] G. Saracco, C. Badini, N. Russo, V. Specchia, Development of catalysts based on pyrovanadates for diesel soot combustion, Appl. Catal. B: Environ. 21 (1999) 233–242.

[7] J. Oi-Uchisawa, A. Obuchi, R. Enomoto, S.T. Liu, T. Nanba, S. Kushiyama, Catalytic performance of Pt supported on various metal oxides in the oxidation of carbon black, Appl. Catal. B: Environ. 26 (2000) 17–24.

[8] J. Oi-Uchisawa, S.D. Wang, T. Nanba, A. Ohi, A. Obuchi, Improvement of Pt catalyst for soot oxidation using mixed oxide as a support, Appl. Catal. B: Environ. 44 (2003) 207–215.

[9] J. Kaspar, P. Fornasiero, M. Graziani, Use of CeO_2-based oxides in the three-way catalysis, Catal. Today 50 (1995) 285–298.

[10] J. Lahaye, S. Boehm, P. Chambrion, P. Ehrburger, Influence of cerium oxide on the formation and oxidation of soot, Combust. Flame 104 (1996) 199–207.

[11] H. Sobukawa, Development of Ceria–Zirconia solid solutions and future, R&D Rev. Toyota CRD 37 (1998) 1–5.

[12] Suda, H. Sobukawa, T. Suzuki, Synthesis of Ceria–Zirconia solid solution and its performance as catalytic promoter, R&D Rev. Toyota CRDL 37 (1998) 3–12.

[13] L. Zhu, X.Z. Wang, Z.P. Hao, Catalytic performance of Ce/Zr oxides catalysts for soot combustion, J. Rare Earths. 22 (2004) 844–848.

[14] Z. Zhao, X.G. Yang, Y. Wu, A comparative study if Ni-based perovskite-like mixed catalysts for direct decomposition of NO, Appl. Catal. B. Environ. 8 (1996) 281–297.

[15] B. Dernaika, D. Uner, A simplified approach to determine the activation energies of uncatalyzed and catalyzed combustion of soot, Appl. Catal. B: Environ. 40 (2003) 219–229.

[16] P. Fornasiero, E. Fonda, R. Di Monte, G. Vlaic, J. Kaspar, M. Graziani, Relationships between structural/textural properties and redox behavior in $Ce_{0.6}Zr_{0.4}O_2$ mixed oxides, J. Catal. 187 (1999) 177–185.

[17] P. Fornasiero, G. Balducci, R. Di Monte, J. Kaspar, V. Sergo, G. Gubitosa, A. Ferrero, M. Graziani, Modification of the redox behaviors of CeO_2 induced by structural doping with ZrO_2, J. Catal. 164 (1996) 173–183.

[18] J.P.A. Neeft, T.X. Nijhuis, E. Smakman, M. Makkee, J.A. Moulijn, Kinetic of the oxidation of diesel soot, Fuel 12 (1997) 1129–1136.

[19] T. Inui, T. Otowa, Y. Takegami, Enhancement of oxygen transmission in the oxidation of active carbon by the composite catalyst, J. Catal. 76 (1982) 84–92.

[20] R.T.K. Baker, J.J. Chludzinski Jr., Catalytic gasification of graphite by chromium and copper in oxygen, steam and hydrogen, Carbon 19 (1981) 75–82.

[21] G. Mul, F. Kapteijn, J.A. Moulijn, Catalytic oxidation of model soot by metal chlorides, Appl. Catal. B: Environ. 12 (1997) 33–47.

[22] A. Galtayries, R. Sporken, J. Riga, G. Blanchard, R. Caudano, XPS comparative study of ceria/zirconia mixed oxides: powders and thin film characterization, J. Electron. Spectrosc. Relat. Phenom. 88-91 (1998) 951–956.